

X-ray absorption of cadmium in the *L*-edge regionJ. Padežnik Gomilšek,¹ A. Kodre,^{2,3} I. Arčon,^{4,3,5} and G. Bratina⁴¹*Faculty of Mechanical Engineering, University of Maribor, Smetanova 17, SI-2000 Maribor, Slovenia*²*Faculty of Mathematics and Physics, University of Ljubljana, Jadranska 19, SI-1000 Ljubljana, Slovenia*³*J. Stefan Institute, Jamova 39, SI-1000 Ljubljana, Slovenia*⁴*University of Nova Gorica, Vipavska 13, SI-5000 Nova Gorica, Slovenia*⁵*Centre of Excellence Low-Carbon Technologies (CO NOT), Hajdrihova 19, SI-1000 Ljubljana, Slovenia*

(Received 4 October 2011; published 11 November 2011)

Atomic x-ray absorption of cadmium in the energy region of *L* edges was measured on the vapor of the element, in parallel with the absorption of Cd metal foil. Ionization thresholds of the three subshells are determined from the edge profiles, through the energies of pre-edge resonances and indium optical levels in the $Z + 1$ approximation. A purely experimental result, without extraneous data and with an accuracy of 0.2 eV, is the energy difference between the pre-edge resonance and the threshold energy of the metallic state. Some multielectron-excitation resonances are identified within 30 eV above the edges. The metal foil absorption is used for absolute determination of Cd absorption coefficient.

DOI: [10.1103/PhysRevA.84.052508](https://doi.org/10.1103/PhysRevA.84.052508)

PACS number(s): 32.30.Rj, 32.80.Aa

I. INTRODUCTION

Since x-ray absorption is essentially an atomic process, the absorption cross section of a compound substance is, to a good approximation, a sum of contributions of constituent elements. In the broad view, the elemental cross sections are only weakly dependent on the chemical or allotropic state of the element. They are monotonously decreasing functions of photon energy, with sharp increases—the absorption edges—at the ionization thresholds of consecutive electron shells. Small deviations from the general smooth decrease with energy are limited to the vicinity of absorption edges: they are caused either by the structure of the atomic neighborhood (XAFS—x-ray absorption fine structure) or by the internal processes in the atom (MPE—multielectron photoexcitations). The elemental cross section should, in principle, be measured and tabulated for the free-atom state of the element, representing the pure atomic absorption, free of XAFS, and directly comparable to quantum-mechanical calculations of the atomic cross section. The free-atom state, with the exception of monatomic noble gases, is not readily available for the experiment. It has only been prepared by vaporization of some volatile metals. For wide-range absorption data, where XAFS and MPE can be neglected, the standard allotropic form of an element, as, e.g., the metallic form of many elements, is regularly used as an absorption sample.

Following the seminal experiments on noble gases [1–3], atomic x-ray absorption has been measured on most volatile metals, i.e., those with a boiling point below ~ 1000 °C. The *K*-edge profiles and the collective MPE excitations have been extensively investigated [4–9]. The *L*-edge energy region has received much less attention due to the considerably more demanding experiments in the softer energy range: in addition to Xe [3,10], only the absorption in Cs and Hg vapors has been studied [11,12] in the wider *L* region. Edge profiles of Ba and Hg [13] were analyzed for excitations into the states below ionization threshold; in an experiment involving temperatures up to 2200 °C atom-to-metal edge shifts of several rare-earth metals (Ce, Sm, Gd, and Er) were studied [14].

X-ray absorption in metals has already been thoroughly studied in the early days of x-ray absorption spectroscopy since perfectly homogenous high-quality absorption specimens with optimum thickness of the order of 10 μm can be prepared with routine mechanical procedures. The *K* edges of metals are often used as intermediary standards for the calibration of the energy scale of x-ray monochromators, allowing an accuracy of ~ 0.1 eV or better [15,16]. The data from the softer x-ray region of *L* edges is again scarcer. The optimum thickness of a foil with *L* edges in the region of 3–5 keV is in the 1 μm range, which may be readily available only for extremely ductile metals such as silver or tin. With evaporated thin layers, particular care is required to achieve the necessary homogeneity and uniform density of the sample.

We have measured the absorption in Cd vapor and in a thin layer of Cd metal in the energy region of *L* edges, from 3400 to 4400 eV. A comparison of the two sets of data provides some results of metrological interest, notably the continuum threshold energies. The *L*-edge profiles and accompanying MPE are discussed and compared to the *K*-edge data [8] of Cd and Zn and the *L*-edge data of Hg [11,17]. Absolute cross-section data are extracted. The atomic *L*-edge absorption of Cd has not been reported before, but a measurement on *L*-edge profiles of an evaporated metallic Cd target has been published by Nordfors and Noreland [18].

II. EXPERIMENT

X-ray absorption of cadmium vapor in the energy region of *L* edges was measured at the beamline A1 of Hasylab, DESY. A preliminary test showed that the experiment was, due to the low energy of the Cd *L* region, extremely demanding but feasible. The definite data were obtained using the two-crystal Si 111 monochromator with a resolution of ~ 0.7 eV. As in earlier low-energy atomic absorption experiments on potassium *K* edge and cesium *L* edges [19,21], the vapor was contained in a 10-cm-long stainless-steel absorption cell with 50 μm beryllium windows, heated to 800 °C in a tubular oven with a protecting He atmosphere. The intensity of the beam was measured with three 10-cm-long ionization detectors, filled

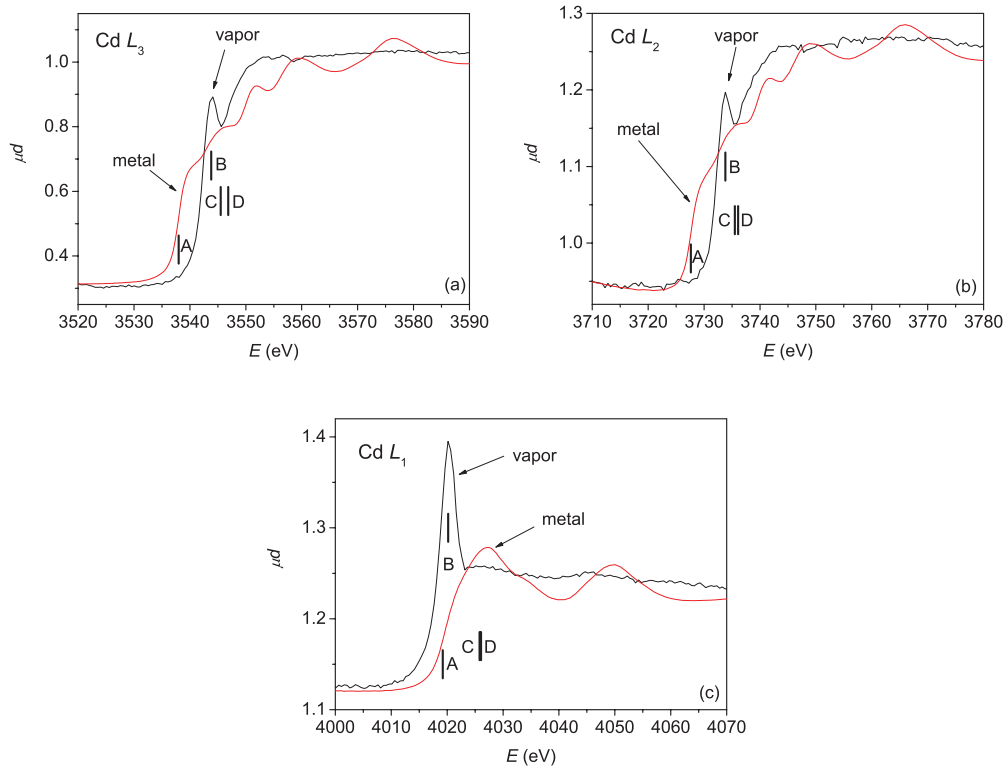


FIG. 1. (Color online) A comparison of Cd L edges in vapor and metal. The vapor attenuation is renormalized to the value of the metal at both extreme ends of the measured interval. A, continuum threshold in metal; B, edge resonance in vapor; C, atomic threshold derived from experiment (see text), and D, NIST atomic threshold value [20].

with 180, 1000, and 1000 mbar of nitrogen. Owing to the high quality of the beam at the A1 station, the absorption in the entire energy region was determined with a uniform accuracy. The energy scale of the monochromator was calibrated with a parallel measurement of $1\ \mu\text{m}$ Ag foil and an improvised Cd metal target, prepared from Cd powder on scotch tape.

The preparation of a proper Cd metal absorber with optimum thickness in the L -edge region is not straightforward since Cd ductility is poor. When a rolled thin foil is not available, an evaporated target is generally the next best choice for absolute absorption measurement. It should be noted that absorbers with suboptimum thickness can still be used since the accuracy of the measured cross section decreases only in proportion to the thickness. It is the homogeneity over the area, however, that is difficult to maintain. For too thick absorbers, on the other hand, the higher harmonics prevail in the transmitted beam, leading to significant systematic errors.

Cd metal absorption samples were deposited as thin layers on $3\ \mu\text{m}$ Al substrate in a vacuum evaporation chamber with a base pressure of 1×10^{-6} Torr, using the mask 11.2×13.2 mm. A resistively heated Ta boat was used to heat a piece of solid Cd (Riedel-de-Haën, purity 99.9%), and the thickness of the layers was monitored *in situ* by a quartz thickness monitor. A typical growth rate of 10 nm/min was employed. Prior to evaporation the material was thoroughly degassed. During deposition the substrate was at room temperature.

The L -edge absorption of the Cd metal sample was measured at the XAFS station of ELETTRA in the transmission detection mode. In the beam from Si(111) double-crystal monochromator with 0.5 eV resolution at 3.5 keV, higher-order

harmonics were suppressed by detuning the crystals to 40% of the rocking curve maximum. The gas fillings of the three 30-cm-long ionization detectors optimized for the energy range of 3400 to 4500 eV were 85, 460, and 880 mbar N_2 , respectively, all topped up with He to 2000 mbar. The energy calibration was maintained with a simultaneous absorption measurement on $2\text{-}\mu\text{m}$ -thick Sn metal foil.

For absolute determination of the absorption cross section, the mass of the Cd metal sample was determined using standard atomic absorption spectroscopy (AAS) with a VARIAN AA240 spectrometer. The sample was digested using concentrated hydrochloric acid, evaporating until dry three times in succession, and diluted with 0.1 M nitric acid in purified water. The digestion procedure yielded a clear solution that was used in flame atomization mode. The result of the analysis for the mass of the sample was 1.47 mg with an estimated accuracy of 6%.

III. ANALYSIS

A. L edges

The profile of an edge in atomic absorption represents a most stringent test of atomic models, as, e.g., various self-consistent atomic calculations. The basic parameter of an edge is the continuum threshold energy. In metals, the parameter is defined as Fermi level, determined as the point of the steepest slope of the edge profile. The simple definition is extremely helpful in practical spectroscopic work, providing reliable local calibration points for monochromator energy scale. In our experiment, the scale is defined jointly by L

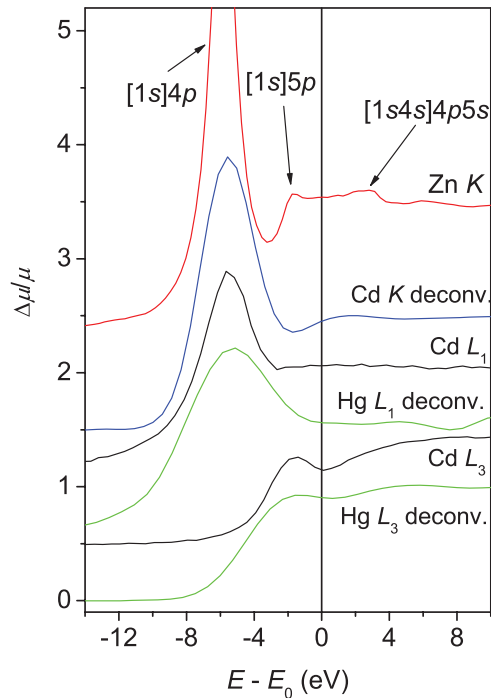


FIG. 2. (Color online) A comparison of homologs: Cd and Hg L edges, Zn and Cd K edges, aligned to respective continuum thresholds. Cd K and Hg L edges are sharpened by deconvolution.

edges of metallic Cd, Ag, and Sn. We will adopt the scale with the L_3 edge of Cd metal at 3538.0 eV, in accord with many practical x-ray tables and right between the two values (experimental direct and combined) of the comprehensible NIST tables [20].

In atomic absorption, on the other hand, the threshold is masked by a preceding progression of ever smaller and ever denser discrete absorption lines to unoccupied orbitals of which only a few initial ones can be discerned. Teodorescu [21] has shown that an apparent edge is observed at the position of the first unresolved discrete line.

In Cd L -edge profiles, only one resonance is resolved, the transition to the $[2s]5p$ or the $[2p]5d$ state. The energy of the resonance is a well-defined experimental parameter, and the threshold energy can be reconstructed from it. Another energy parameter, useful in testing theoretical models, is the shift between the metallic and atomic edge threshold. In its place, a purely experimental parameter, free of extraneous data and independent of the energy calibration, can be used: the energy difference ΔE_{rm} between the atomic resonance and the metallic edge. Measured in a single energy scan, it can be determined with high accuracy, estimated to ± 0.2 eV.

The profiles of the L_3 and L_2 edges [Figs. 1(a) and 1(b)] are practically identical in the relative energy scale, taking into account the jump ratio 2:1. The L_1 jump [Fig. 1(c)] is ~ 5 times smaller than that of L_3 , the profile has a different shape, similar to that of the Cd K edge (Fig. 2) after the deconvolution procedure enabled by the high quality of the K -edge data, whereby the effective width is brought closer to L -edge widths. The potential felt by the electron excited to an unoccupied orbital depends only weakly on the principal

number of the inner shell with vacancy. Hence, the relative energies of pre-edge resonant states, as well as those of multiple excitations are practically the same in K - and L_1 -edge spectra. Even in congener elements with a corresponding outer-shell configuration, i.e., in the Zn K edge and Hg L_1 edge where an s -type inner vacancy is also combined with a $nd^{10}(n+1)s^2$ valence configuration, a similar overall shape can be recognized, albeit on a slightly compressed or expanded energy scale. The smaller lifetime width of Zn K vacancy makes all resonances sharper and higher, while in Hg L_1 with a large width, the elements of the edge profile are only recognized after deconvolution. The Cd $L_{2,3}$ edges can only be compared to corresponding Hg L edges.

In the L_1 and K edges included in the above comparison the prominent pre-edge resonance—the “white line”—is quite well separated from the ionization threshold. It is the $[(1,2)s](4,5,6)p$ state involving the orbital which is just getting filled in the subsequent elements and is thus relatively strongly bound. The better resolution of the Zn K edge even reveals the next resonance in the Rydberg series, the $[1s]5p$ line 4.0 eV higher in energy. In Cd L_1 , the corresponding line is indicated just by the sharp turn of the white line into the edge. In $L_{2,3}$ edges, on the other hand, the d levels involved in the final state of the excitation will only get filled in the subsequent element period ending with the congener Hg: they lie very close to continuum and so the white line is much closer to the continuum threshold.

To determine the position of the atomic threshold, the edge profile is fitted by a combination of a Lorentz resonance and an arctan edge, convoluted by a Gaussian instrumental width. Since the edge is an apparent edge, an accumulation of Rydberg series, its energy parameter is not the threshold, and neither are the two connected by a simple relation. Instead, the indisputable energy of the Lorentzian is used to determine the threshold. In the L_1 edge, with a relatively large and well-separated resonance, the energy is determined with an accuracy of 0.2 eV. In the L_2 and L_3 edges with the resonance leaning on the slope of the edge, the accuracy is estimated to 0.3 eV. In all edges, the fit gives the Gaussian instrumental width of ~ 1 eV.

With the energy of the metal threshold set by the definition of the energy scale, the parameter ΔE_{rm} is directly determined by the resonance energy. The atomic threshold, on the other hand, cannot be derived from the absorption experiment alone: a theoretical self-consistent-field calculation can be used to determine the energy difference between the resonance and the proper edge, invisible in the experiment. It is the energy difference between the configurations $[2(s,p)]$ and $[2(s,p)]5(p,d)$. The difference can be determined with satisfactory precision, even if the full configuration energies may be off for several eV.

Another useful approach, known as the “ $Z + 1$ approximation,” is based on the already invoked independence of the atomic periphery on the core vacancy. In the $Z + 1$ atom, the increased nuclear charge has the same effect on the valence configuration as the core vacancy in the Z atom. Consequently, the relative energies of excited states in Cd with an inner-shell vacancy and the optical levels of the subsequent neutral In atom with its outer electron in the same orbital should be very close. In the same sense, the congener pairs Zn-Ga in Hg-Tl

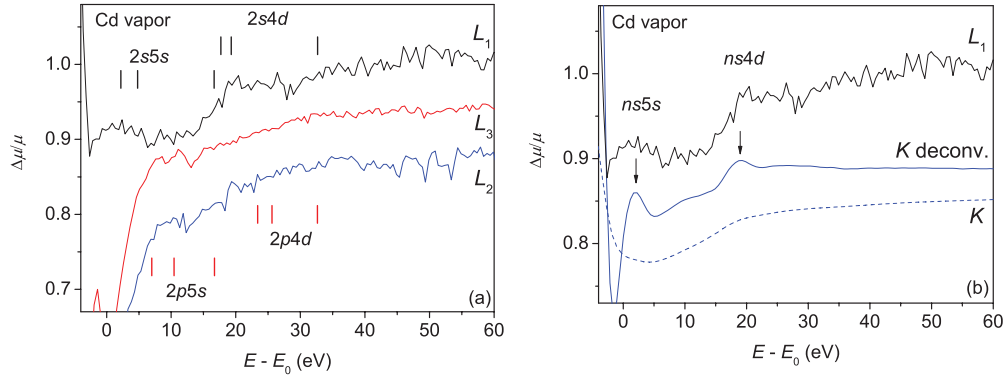


FIG. 3. (Color online) Cd L multielectron excitations in the relative energy scale: (a) comparison of subshell MPE, (b) L_1 edge and the corresponding segment of the Cd K spectrum with its deconvolution.

can be included in a comparison of the merits of the two approaches.

Single-configuration Dirac-Fock (DF) [22] calculation sets Zn[1s]4p_{3/2} at 5.4 eV below continuum, and Cd[2s]5p_{3/2} at 5.0 eV. Practically identical values are calculated for the corresponding optical levels in $Z + 1$ Ga and In. Experimental values for these levels [23], however, are 5.9 and 5.5 eV, respectively. The same miss of ~ 0.5 eV is also found in congeners with np^1 configuration, Al and Tl. The higher members of the Rydberg series in these elements, on the other hand, show very good agreement of experimental and DF values. Thus we conclude that the 0.5 eV difference is due to configuration interaction in the lowermost resonant excitation. Indeed, in Al, the only case where the configuration-interaction (CI) calculation can be brought to convergence directly, the $\sim 4\%$ admixture of the [ns]nd state yields a 0.6 eV decrease in energy, just 0.1 eV above the experimental value. With a more comprehensive CI calculation in In [24], including a much richer set of configurations, the residual is only 0.02 eV. Apparently, in all congener elements with a single electron in np , the ground state interacts with the $nsnpnd$ configuration, i.e., the state with one of the ns electrons moved to nd , leading to a substantial energy decrease. The same combination of configurations is encountered in the excited state of the preceding elements, Cd in our case, leading to a decrease in the $1,2s \rightarrow np$ transition energy.

The resonances at the L_2 and L_3 edges of Cd belong to excitation from $2p$ to $6s$ and $5d$ orbitals. These lie high above

the filled orbitals, close to the continuum, only 2.5 and 1.5 eV, respectively, below the threshold, as estimated by a marginally stable Hartree-Fock (HF) calculation [25]; the corresponding levels in the In optical spectrum are 2.8 and 1.7 eV below continuum. The 1 eV difference is too small to allow a reliable identification of two lines. Judging by a similar resolved case in Xe $L_{2,3}$ [26], the probability of transition into $6s$ is negligible in comparison with that into $5d$.

Following these arguments, we conclude that the best choice for evaluation of the continuum threshold in Cd L edges from the energy of the edge resonances is $Z + 1$ approximation from corresponding optical levels in In: 5.5 eV for L_1 and 1.7 eV for $L_{2,3}$ (Table I), introducing an additional uncertainty of 0.2 eV. The resulting threshold values are satisfactorily close to the NIST data; in fact, within the error bars of the latter for the L_1 edge.

B. Multielectron excitations

Using the edge-profile model as a baseline, some fingerprints of coexcitation of electrons from the valence and subvalence shells in the main photoabsorption process can be identified in a wider edge region within 30 eV above the edge. The positions of the candidate features are compared with HF energies of doubly excited states [Fig. 3(a)]. In addition to matching with theoretical energies, the L_1 MPE features can be best identified in comparison with the K -edge features of Cd, recovered in deconvolution. There, small resonances of [1s5s] and [1s4d] states together with a small edge of the [1s5s] group are clearly visible: in Cd L_1 absorption small

TABLE I. The basic energy parameters of the Cd L edges: the energy of the leading atomic resonance and of the continuum threshold in the metallic state, with the difference ΔE_{rm} , independent of energy calibration; the $Z + 1$ estimate of the resonance energy relative to atomic ionization threshold ΔE_{ir} , and the subsequent atomic threshold values. The error interval of the experimental threshold values is a combination of uncertainties of experimentally determined parameters and the estimated error of the accepted energy calibration 0.5 eV.

	Experimental values		Energy shifts		Atomic threshold	
	$E(2l \rightarrow 5l')$ (eV)	$E(2l \rightarrow \epsilon l')$ (eV)	ΔE_{rm} (eV)	ΔE_{ir} (eV)	Expt. (eV)	NIST ^a (eV)
L_3	3543.8(3)	3538.0	5.8(3)	1.7(2)	3545.5(9)	3546.84(32)
L_2	3733.8(3)	3727.6(2)	6.2(3)	1.7(2)	3735.5(9)	3736.10(39)
L_1	4020.3(2)	4019.2(3)	1.1(2)	5.5(2)	4025.8(8)	4026.07(98)

^aReference [20].

humps can be recognized at approximately the same relative energies [Fig. 3(b)].

In Fig. 3(a), the coexcitations at the L_1 and $L_{2,3}$ edges are compared with the help of HF energy estimates. For each of the $5s$ and $4d$ groups the HF energies show, in succession, the lowermost level for each type of double excitation, the excitation-ionization, and finally the double ionization. The relative energies of L_3 and L_2 coexcitations are greater than those of the corresponding L_1 coexcitations. The lowermost MPE [$2s5s$] $5p6s$ in L_1 is only 2 eV above the threshold, and 7 eV in L_3 . The difference vanishes by the double-ionization end points of a series since the coionization energy depends only weakly on the inner vacancy. In spite of the large noise a sharp feature can be discerned at the start of the $4d$ series in L_1 but not in L_3 . With the help of K -edge analogy it is recognized as [$2s4d$] $5p5d$ resonance. The fact that the nd MPE series generally mimic the profile of the main edge has been observed and explained before [4,27].

C. Absolute determination of cross section

In XAFS analysis with synchrotron light, x-ray-absorption spectra of substances are routinely determined with eV resolution and high relative accuracy. The analysis is not susceptible to smooth additive contributions or to arbitrary intensity factors. The absolute measurement, necessary for tabulation of the mass absorption coefficient, however, is seldom performed, requiring special attention and preparation. As discussed before [8] the check of the exponential decrease of transmitted beam intensity with sample thickness is extremely important, guarding against the systematic errors due to sample inhomogeneity and higher harmonics in the beam. The main source of uncertainty of the results, as a rule, is the determination of the surface density of the sample. Relatively good results within 2% error are obtained for gaseous samples and rolled metal foils, relying on local homogeneity.

The determination of the sample density in the Cd vapor experiment would be extremely demanding. Instead, the independence of the cross section on the chemical form of the element in the regions far from the edges is exploited, and the absorption is measured on the metal Cd layer evaporated on the Al foil. The result of a measurement is the attenuation $A = \mu d = \ln(I_0/I_1)$, the logarithm of the ratio of the incident and transmitted beam intensity. Attenuations of a single and a double (folded) Cd layer, $A_1(E)$ and $A_2(E)$, respectively, are taken with a uniform 5 eV step over the entire interval from 3400 to 5000 eV. In the same way, the spectrum $A_0(E)$ of the Al foil without Cd is measured.

The attenuations in the three spectra at every photon-energy point E should, in an ideal case, remain in a linear relation $aA_0(E) + bA_1(E) + cA_2(E) = 0$, with a, b, c constant over the entire interval. Systematic deviation, however, was found: it was attributed to the third-order harmonics in the incident beam, the vestige after the suppression with the working point at 40% of the rocking-curve peak. A model of the third-order contribution as a function of monochromator energy was constructed, taking into account the absorption along the beam path and the efficiency of the detectors. The contributions, appropriate for the target thickness, were removed from the

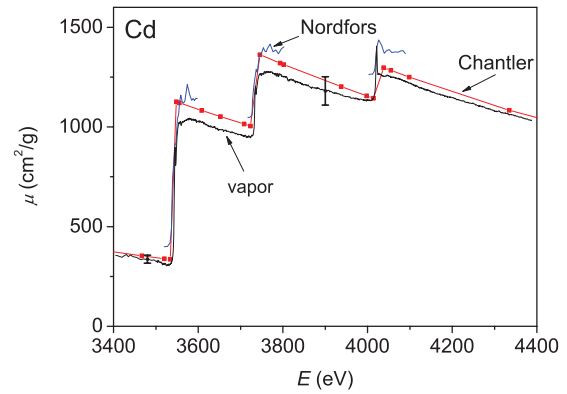


FIG. 4. (Color online) Mass absorption coefficient of Cd in the L region; the error bars show a 6% uncertainty level.

respective transmitted beam intensities, defining the corrected attenuation $A'_i(E)$. The unknown intensity factor of the third-order beam was adjusted to the value giving the least variation of the ratio between the attenuations in the double and single layers, $A'_2(E)$ and $A'_1(E)$. Indeed, a completely random residual of the ratio was achieved over the interval. The optimum ratio was not exactly 2, as expected for a folded sample, but rather 1.89. The deviation can be used as a measure of the overall inhomogeneity of the layer, but it does not affect the accuracy of the measured attenuation values directly. In the attenuation of the folded sample an average over the inhomogeneity is already included. The overall accuracy of the attenuation itself is estimated to 1%.

The main contribution to the uncertainty interval of the mass absorption coefficient is, as usual, the uncertainty of the mass density of the sample. The mass of Cd determined by the quantitative analysis is divided by the area of the mask used in the evaporation of the sample. For the small mass, the estimated accuracy is 6% and this is also the accuracy of the mass absorption coefficient, obtained when the vapor attenuation is renormalized to the metal attenuation at both extreme ends of the measured interval. The graphic presentation of the data in Fig. 4 seems appropriate for the rather large uncertainty.

Our result agrees well with the values from the Nordfors and Noreland [18] experiment in the entire L region, after a constant difference of ~ 100 cm^2/g is taken into account. We believe that the check of exponential attenuation through single and double foils increases the reliability of our experiment. The values from the recent x-ray-absorption compilation [28] agree with our data well below the L_3 edge and show an improving convergence high above L_1 , but stay low in the region between the edges. Jitschin and Stotzel [29] have already observed that the calculated cross sections are consistently high in the region of the L edges, and their slopes too steep. The differences were ascribed to electron correlations.

IV. CONCLUSION

The atomic absorption measured on the vapor of an element is, by definition, also the exact “atomic absorption background” for the extended x-ray-absorption fine-structure

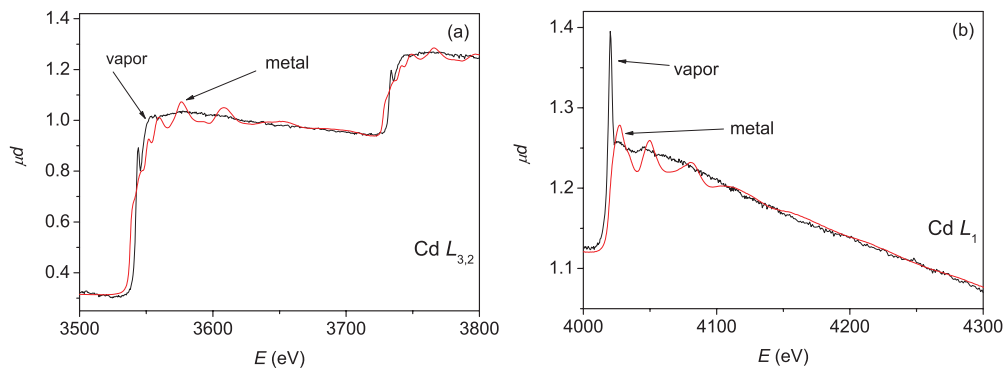


FIG. 5. (Color online) The atomic absorption of Cd vapor and metal, normalized as in Fig. 1; beyond the XANES region, within ~ 40 eV of the edge, atomic absorption is the exact atomic background for the L -edge EXAFS of Cd metal.

(EXAFS) analysis in the sense of Fig. 5, where it is applied to the EXAFS spectrum of the metal itself. It represents a standard against which to judge the adequacy of the spline approximation of standard EXAFS analysis software, and which should be used in critical cases of samples with very low structural signals. Although for Cd itself with a mere 190 eV separation of the L_3 and L_2 edges, K -shell EXAFS is preferably used for structure analysis, our measurement on the Cd L region may be helpful in construction of model atomic backgrounds for the adjacent region of elements, providing one of the lowest- Z atomic absorption spectra in the L -shell region, accessible with the present x-ray-absorption technique.

ACKNOWLEDGMENTS

This work was supported by the Slovenian Research Agency (program P1-0112) and by DESY and the European Community's Seventh Framework Programme (FP7/2007-2013) ELISA (European Light Sources Activities) under grant agreement No. 226716. Access to synchrotron radiation facilities of HASYLAB (project II-20080058 EC) and XAFS beamline of ELETTRA is acknowledged. We would like to thank A. Webb, R. Chernikov, and E. Welter of HASYLAB, and G. Aquilanti and L. Olivi of ELETTRA for expert advice on beamline operation, as well as M. Šala, for the quantitative determination of the Cd mass in the metal sample.

- [1] R. D. Deslattes, R. E. LaVilla, P. L. Cowan, and A. Henins, *Phys. Rev. A* **27**, 923 (1983).
- [2] S. J. Schaphorst, A. F. Kodre, J. Ruscheinski, B. Crasemann, T. Åberg, J. Tulkki, M. H. Chen, Y. Azuma, and G. S. Brown, *Phys. Rev. A* **47**, 1953 (1993).
- [3] K. Zhang, E. A. Stern, J. J. Rehr, and F. Ellis, *Phys. Rev. B* **44**, 2030 (1991).
- [4] A. Kodre, I. Arcon, J. Padežnik Gomilšek, R. Preseren, and R. Frahm, *J. Phys. B* **35**, 3497 (2002).
- [5] J. P. Gomilšek, A. Kodre, I. Arcon, and R. Preseren, *Phys. Rev. A* **64**, 22508 (2001).
- [6] J. P. Gomilšek, A. Kodre, I. Arcon, and M. Hribar, *Phys. Rev. A* **68**, 042505 (2003).
- [7] A. Mihelic, A. Kodre, I. Arcon, J. Padežnik Gomilšek, and M. Borowski, *Nucl. Instrum. Methods Phys. Res. B* **196**, 194 (2002).
- [8] A. Kodre, J. Padežnik Gomilšek, A. Mihelic, and I. Arcon, *Rad. Phys. Chem.* **75**, 188 (2006).
- [9] U. Arp, B. M. Lagutin, G. Materlik, I. D. Petrov, B. Sonntag, and V. L. Sukhorukov, *J. Phys. B* **26**, 4381 (1993).
- [10] I. Arcon, A. Kodre, M. Stuhec, D. Glavic-Cindro, and W. Drube, *Phys. Rev. A* **51**, 147 (1995).
- [11] A. Filipponi, L. Ottaviano, and T. A. Tyson, *Phys. Rev. A* **48**, 2098 (1993).
- [12] A. Kodre, J. Padežnik Gomilšek, I. Arcon, and G. Aquilanti, *Phys. Rev. A* **82**, 022513 (2010).
- [13] O. Keski-Rahkonen, G. Materlik, B. Sonntag, and J. Tulkki, *J. Phys. B* **17**, L121 (1984).
- [14] G. Materlik, B. Sonntag, and M. Tausch, *Phys. Rev. Lett.* **51**, 1300 (1983).
- [15] I. Arcon, J. Kolar, A. Kodre, D. Hanzel, and M. Strlic, *X-Ray Spectrom.* **36**, 199 (2007).
- [16] R. Dominko, I. Arcon, A. Kodre, D. Hanzel, and M. Gaberscek, *J. Power Sources* **189**, 51 (2009).
- [17] R. Preseren, I. Arcon, A. Kodre, and R. Frahm, *HASYLAB am DESY Jahresbericht* **1995**, 57 (1995).
- [18] B. Nordfors and E. Noreland, *Ark. Fys.* **20**, 1 (1969).
- [19] J. Padežnik Gomilšek, A. Kodre, I. Arcon, and V. Nemanic, *Nucl. Instrum. Methods Phys. Res. B* **266**, 677 (2008).
- [20] R. D. Deslattes, E. G. Kessler Jr., P. Indelicato, L. de Billy, E. Lindroth, J. Anton, J. S. Coursey, D. J. Schwab, C. Chang, R. Sukumar, K. Olsen, and R. A. Dragoset, *X-Ray Transition Energies*, version 1.2 (National Institute of Standards and Technology, Gaithersburg, MD, 2005). Available at [<http://physics.nist.gov/XrayTrans>] (last accessed July 25, 2011).
- [21] C. M. Teodorescu, R. C. Karnatak, J. M. Esteva, A. El Afif, and J.-P. Connerade, *J. Phys. B* **26**, 4019 (1993).
- [22] K. G. Dyall, I. P. Grant, C. T. Johnson, F. A. Parpia, and E. P. Plummer, *Comput. Phys. Commun.* **55**, 425 (1989).
- [23] Yu. Ralchenko, A. E. Kramida, J. Reader, and NIST ASD Team, *NIST Atomic Spectra Database*, version 4.0 (National Institute of Standards and Technology, Gaithersburg, MD, 2010). Available at [<http://physics.nist.gov/asd>] (last accessed July 25, 2011).
- [24] M. Das, R. K. Chaudhuri, S. Chattopadhyay, and U. S. Mahapatra, *J. Phys. B* **44**, 065003 (2011).

- [25] C. Froese Fischer and G. Tachiev, *MCHF/MCDHF Collection*, version 2 (National Institute of Standards and Technology, Gaithersburg, MD, 2011). Available online at [<http://physics.nist.gov/mchf>]
- [26] M. Breinig, M. H. Chen, G. E. Ice, F. Parente, B. Crasemann, and G. S. Brown, *Phys. Rev. A* **22**, 520 (1980).
- [27] J. A. Solera, J. Garcia, and M. G. Proietti, *Phys. Rev. B* **51**, 2678 (1995).
- [28] C. T. Chantler, K. Olsen, R. A. Dragoset, J. Chang, A. R. Kishore, S. A. Kotochigova, and D. S. Zucker, *X-Ray Form Factor, Attenuation, and Scattering Tables* (National Institute of Standards and Technology, Gaithersburg, MD, 2001). Available at [<http://www.nist.gov/pml/data/ffast/index.cfm>] (last accessed July 2011).
- [29] W. Jitschin and R. Stotzel, *Phys. Rev. A* **58**, 1221 (1998).